Anal Bioanal Chem (2014) 406:851–858
DOI 10.1007/s00216-013-7503-z

RESEARCH PAPER

# Highly sensitive determination of ssDNA and real-time sensing of nuclease activity and inhibition based on the controlled self-assembly of a 9,10-distyrylanthracene probe

**Xing Li · Ke Ma · Hongguang Lu · Bin Xu · Zilong Wang · Yan Zhang · Yajun Gao · Lulin Yan · Wenjing Tian**

Received: 24 May 2013 / Revised: 12 September 2013 / Accepted: 11 November 2013 / Published online: 28 November 2013


**Abstract** We report here a fluorescent biosensor for highly sensitive determination of single-stranded DNA (ssDNA) with remarkable fluorescence enhancement and label-free sensing of S1 nuclease activity and inhibition in real time based on ssDNA-controlled self-assembly of a 9, 10-distyrylanthracene (DSA) probe with the aggregation-induced emission (AIE) property, thereby avoiding a sophisticated fabrication process and aggregation-caused quenching (ACQ) effect. Compared with previous technologies, this assay has some advantages. First, since the DSA probe can be synthesized through a simple and effective synthetic route and the sensing technology adopts the unlabelled ssDNA, this biosensor shows advantages of simplicity and cost efficiency. Besides, for the determination of ssDNA, S1 nuclease, and inhibitor, the DSA-based probe provides high sensitivity and a good linear relationship due to the AIE property. As a result, we determined the DNA 24-mer concentration as low as 150 pM, and we are able to detect ssDNA lengths with a linear range from 6mer to 24mer ($R$ = 0.998) as well as DNA 24-mer concentrations with a linear range from 0 to 200 nM ($R$ = 0.998) and S1 nuclease concentrations with a linear range from 6 to 32 U $ml^{-1}$ ($R$ = 0.995), respectively. Moreover, the fluorescent intensity with various concentrations of S1 nuclease becomes highly discriminating after 3–16 min. Thus, it is possible to detect nuclease activity within 3–16 min, which demonstrates another advantage of a quick response of the present biosensor system.

**Keywords** 9,10-Distyrylanthracene probe · Aggregation-induced emission · Aptasensor · Nuclease activity and inhibition · Self-assembly

## Introduction

DNA or RNA cleavage reaction catalyzed by restriction or nonrestriction nucleases is of significant importance in many biological fields ranging from biotechnology to pharmacology as well as in biological processes involving replication, genetic recombination, DNA repair, molecular cloning, genotyping, and mapping [1–6]. Traditional nuclease activity assays such as gel electrophoresis, radioactive labeling, high-performance liquid chromatography (HPLC), sedimentation, colorimetric determination, enzyme-linked immunosorbent assay (ELISA), and mass spectrometry (MS) are powerful methods for analyzing the precise structural features of DNA and nuclease activity, but they are time-intensive, laborious, DNA-consuming, discontinuous, or usually requiring isotope labeling [7–14]. What is more, these cleavage assays were mostly designed for the restriction nucleases of double-stranded DNA (dsDNA). Single-strand-specific nucleases are a family of multifunctional enzymes and widespread in living organisms, which exhibit high selectivity for ssDNA and the single-strand regions in dsDNA. It is hence very important to develop simple, rapid, and more convenient technology to monitor single-strand-specific nuclease activities and inhibition, especially for clinical diagnostics, drug

**Electronic supplementary material** The online version of this article (doi:10.1007/s00216-013-7503-z) contains supplementary material, which is available to authorized users.

X. Li · K. Ma · H. Lu · B. Xu (✉) · Z. Wang · Y. Zhang · Y. Gao · L. Yan · W. Tian (✉)
State Key Laboratory of Supramolecular Structure and Materials, Jilin University, 2699 Qianjin Avenue, Changchun 130012, China
e-mail: xubin@jlu.edu.cn
e-mail: wjtian@jlu.edu.cn

screening, and bioanalysis. Up to now, based on electron transfer (ET), charge transfer (CT), energy transfer (ET), and excimer/exciplex mechanisms, scientists have developed some fluorescent probes including conjugated polymer, small molecules, and nanoparticles [13, 15–20] to study single-strand-specific nuclease activity, but these probes are compromised by sophisticated fabrication process, fluorophore or functionalizing thiol-labeled DNA, and notorious aggregation-caused quenching (ACQ) effect.

In 2001, Tang's group observed a novel aggregation-induced emission (AIE) effect in 1-methyl-1,2,3,4,5-pentaphenylsilole [21]. In 2006, they later found that tetraphenylethene and its derivatives also showed AIE behavior [22]. The concept of AIE has emerged to be a new signaling mechanism [23–26]. AIE luminophores, which are practically nonluminescent in their solution state but become strongly emissive after aggregation, have developed as not only excellent emitters for the construction of efficient light-emitting diodes but also sensitive bioprobes for sensing [27–39]. However, there is rare report about the real-time monitoring for ssDNA cleavage and nuclease inhibition using AIE luminophores. In order to cover this shortage, our group has developed a series of AIE-active 9,10-distyrylanthracene (DSA) derivatives and successfully applied them for pH sensor, $Pb^{2+}$ sensor, biosensor, and bioimaging [40–43]. In this paper, we synthesized an AIE-active DSA derivative, 9,10-bis{4-[2-(*N*,*N*,*N*-triethylammonium)-ethoxy]styryl}anthracene dibromide (BTAESA), through simple and effective synthetic route, and developed the label-free and real-time sensing for ssDNA, nuclease activity, and inhibition based on the controlled self-assembly of the DSA molecule. Given its simplicity, easy operation, and sensitivity of fluorescence, this label-free fluorescent real-time assay will show potential applications in the assay of other nucleases and high-throughput screening of nucleases inhibitors, which show significant importance in modern drug discovery.

## Materials and methods

### Materials and reagents

All reagents and starting materials were analytical grade and used without further purification. Tetrahydrofuran (THF), triethylamine, *N*,*N*′-dimethylformamide (DMF), dimethyl sulfoxide (DMSO), anthracene, potassium *tert*-butoxide ($KO^tBu$), and potassium carbonate were commercially available from Sigma-Aldrich (St. Louis, MO) and were used without further purification.

S1 nuclease was purchased from Sangon Biotechnology Co., Ltd. (Shanghai, China). Adenosine 5′-triphosphate disodium salt ($Na_2ATP$) was purchased from Dingguo Biotechnology Company Limited (Beijing, China). All oligonucleotides including ssDNA 6mer (5′-TGTCTG-3′), ssDNA 10mer (5′-TGTTTTGTCT-3′), ssDNA 15mer (5′-CCAGATAC TCACCGG-3′), ssDNA 20mer (5′-ATCGTATAATGGTT TCGTTC-3′), ssDNA 24mer (5′-CTAACGGAATGTTC ATTCGGTTAG-3′), and ssDNA 32mer (5′-TTACGG AAACGGAATTTATTCGGTATCGGTTA-3′) purified by PAGE method were obtained from Sangon Biotechnology Co., Ltd. (Shanghai, China).

The buffer for nuclease digestion with a pH of 4.6 contained 50 mM sodium acetate and 10 mM zinc sulfate and stored at −20 °C. The dry crystals of oligonucleotides were dissolved in deionized water, and then, the oligonucleotide concentrations were quantified by UV–Vis absorption spectroscopy with the following extinction coefficients ($\varepsilon_{260\ nm}$, $M^{-1}\ cm^{-1}$) for each nucleotide: $A$=15,400, $C$=7,400, $G$=11,500, and $T$=8700. The stock solution of 100 μM oligonucleotides was stored at 4 °C. Tris buffer was adjusted to pH 7.2 with acetic acid. Deionized water (18.2 MΩ/cm resistivity) from a Milli-Q water system was used throughout the experiments.

### Apparatus

The $^1$Hand $^{13}$C NMR spectra were recorded at 298 K on the AVANCZ 500 spectrometer and the Varian Mercury 300 NMR, respectively, with tetramethylsilane (TMS) as the standard. Mass spectra were recorded on the Autoflex speed TOF/TOF system. UV–Vis absorption spectra were recorded on the Lambda 800 Spectrophotometer. The emission spectra were measured with RF-5301PC luminescence spectroscopy. Excitation wavelength was set at 425 nm, and the emission spectra from 445 to 700 nm were collected.

### *Synthesis of BTAESA*

Scheme 1 presents the synthetic route we followed to synthesize BTAESA which was improved according to the literature reports. 9,10-bis[4-(2-Bromoethoxy)styryl]anthracene (BBSA) was synthesized based on the literature reports [41, 44, 45]. Then, a 100 ml round-bottom flask with a magnetic spin bar was charged with 0.28 g of BBSA dissolved in 20 ml of THF and 30 ml of triethylamine. The mixture was heated to reflux and stirred for 3 days. During the period, over 10 ml of water was added at several intervals. The organic solvents and the aqueous solution were evaporated under reduced pressure. After solvent evaporation, the residue was washed with chloroform and acetone and then dried overnight in vacuo at 50 °C. The product (BTAESA) was isolated in 42 % yield. 1H NMR (DMSO-$D_6$, 500 MHz), $\delta$ (TMS, ppm): 8.36–8.39 (m, 4H), 7.99 (d, $J$=16.5 Hz, 2H), 7.83 (d, $J$=8.5 Hz, 4H), 7.55–7.60 (m, 4H), 7.12 (d, $J$=8.5 Hz, 4H), 6.93 (d, $J$=16.5 Hz, 2H), 4.49–4.48 (t, 4H), 3.74–3.72 (t, 4H), 3.43–3.40 (m, 12H), 1.29–1.24 (t, 18H); 13C NMR (DMSO-$D_6$, 75 MHz), $\delta$ (TMS, ppm):

**Scheme 1** Synthetic route of BTAESA

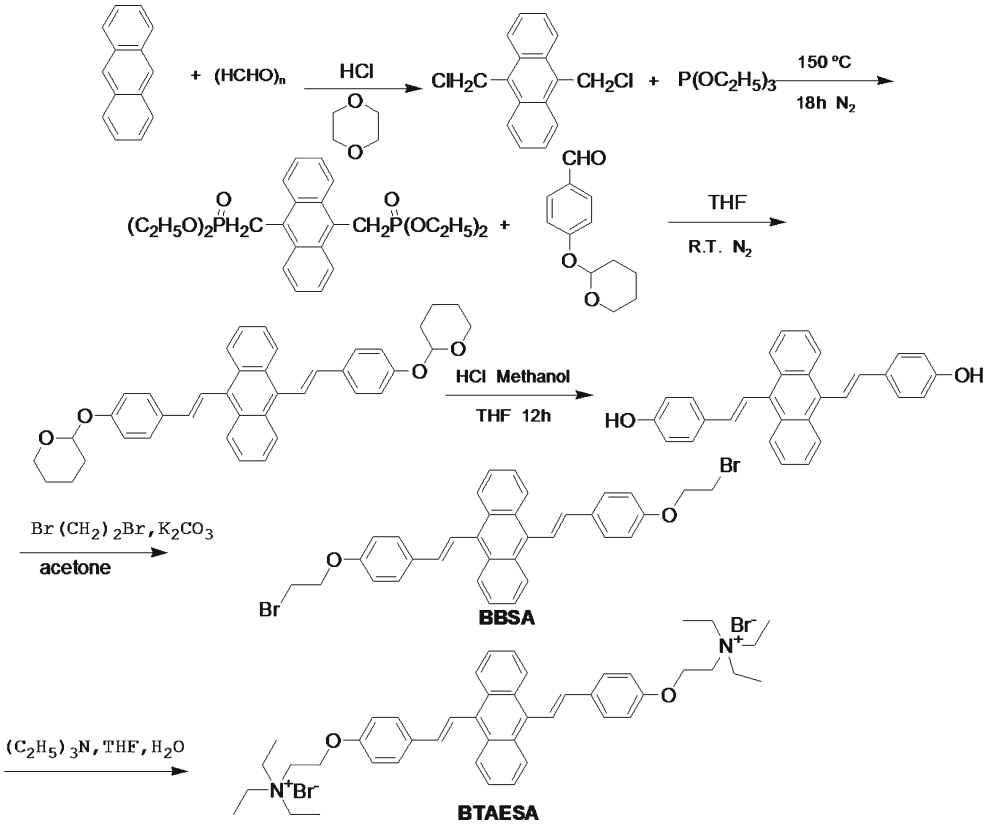


157.92, 137.04, 132.84, 131.00, 129.49, 128.61, 126.65, 125.95, 123.31, 115.42, 61.59, 55.38, 53.31, 7.85. EI-MS *m*/*e* is 335.3 ($[M\text{-}2Br]^{2+}$, calculated as 335.23).

*Fluorescent sensing of DNA by label-free BTAESA*

The same amount ssDNAs (0.4 μM) with a different length ranged from 6mer to 32mer was mixed with BTAESA at a fixed concentration of 1.0 μM in buffer (Tris-HAc, *c* =200 mM, pH=7.2). The mixture was equilibrated for 10 min before spectral measurements, and then, the solutions were excited at 425 nm, and emission spectra were collected from 445 to 700 nm at room temperature.

In addition, a different amount of ssDNA 24mer in the range from 0 to 0.4 μM was mixed with BTAESA at a fixed concentration of 1.0 μM. The mixture was equilibrated for 10 min before spectral measurements, and then, the solutions were excited at 425 nm, and emission spectra were collected from 445 to 700 nm at room temperature.

*Fluorescent sensing of nuclease activity in real time*

The reaction mixture was prepared by mixing 0.4 μM ssDNA 24mer, 1.0 μM BTAESA in the S1 nuclease buffer (2 mM $CH_3COONa$, 15 mM NaCl, 0.1 mM $ZnSO_4$, pH=4.6) at 37 °C. For real-time sensing of the enzyme activity, five solutions containing 6, 8, 12, 16, and 32 U $ml^{-1}$ S1 nuclease in the reaction buffer, respectively, were prepared. The excitation and emission wavelength were chosen at 425 and 552 nm, respectively.

*Monitoring the inhibition effect in real time*

The reaction mixture was prepared by mixing 0.4 μM ssDNA 24mer, 1.0 μM BTAESA, and 32 U $ml^{-1}$ S1 nuclease in the S1 nuclease buffer (2 mM $CH_3COONa$, 15 mM NaCl, 0.1 mM $ZnSO_4$, pH=4.6) at 37 °C. In the experiment of monitoring S1 nuclease inhibition in real time, five solutions containing 0.05, 0.1, 0.2, 0.4, and 1.0 mM $Na_2ATP$ in the reaction buffer, respectively, were prepared. The excitation and emission wavelengths were chosen at 425 and 552 nm, respectively.

## Results and discussion

### Design strategy of real-time sensing of S1 nuclease and inhibition

Figure 1 shows the strategy of the assay for nuclease activity/inhibition. S1 nuclease was chosen as the model enzyme. S1 nuclease is known to be a single-strand-specific endonuclease, which used to hydrolyze selectively ssDNA or RNA to mono- or oligonucleotide fragments [46, 47]. The mechanism of

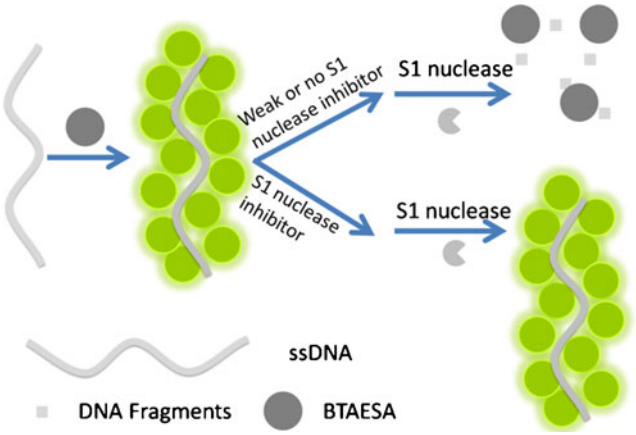


**Fig. 1** Illustration representation of fluorescent sensing for S1 nuclease activity and inhibition screening based on the controlled self-assembly of AIE-active BTAESA probe

sensing includes three steps. Initially, BTAESA is virtually nonfluorescence in buffer solution when in a dispersed state. When ssDNA is added into the solution, the fluorescence of the ensemble would be enhanced. The interactions between BTAESA and ssDNA, including electrostatic and hydrophobic interactions, result in self-assembled aggregation of the probe and ssDNA and further lead to enhanced emission. Upon the addition of S1 nuclease, DNA becomes fragments after reactions. The supramolecular interactions between BTAESA and the fragment would become weak. In this way, the self-assembled aggregation of BTAESA and the fluorescence intensity of the ensemble become dependent on the hydrolysis reaction process of ssDNA with S1 nuclease. In addition, the inhibitors of S1 nuclease can also be monitored because they inhibit the cleavage of ssDNA by the S1 nuclease. Therefore, a label-free and real-time fluorescent nuclease activity assay and nuclease inhibitor screening can be realized using the strategy of the assay based on BTAESA.

## Fluorescent turn-on sensing of DNA

To check the critical length of DNA fragments that can efficiently enhance the fluorescence of the ensemble adduct with BTAESA, the fluorescence spectra of BTAESA in the presence of ssDNA with different base lengths varying from 6mer to 24mer were measured. It was found that the solution pH value had some influence on the performance of the assay (see Electronic Supplementary Material Fig. S1). As the fluorescence intensity increased from pH 4.6 to 7.2, when the pH reached 7.2, the maximum value was obtained. So our results show that pH 7.2 was the optimal pH value used in the current investigation, which is consistent with other reports [48, 49]. Figure 2 displays the plot of the fluorescence intensity of BTAESA (1.0 μM in 20 mM Tris-HAc buffer solution, pH 7.2) versus six selected ssDNA samples with the different lengths at the same DNA concentration (400 nM). Obviously, as displayed in Fig. 2a, the enhancement of BTAESA fluorescence in the presence of short ssDNA such as DNA 6mer can be neglected. The fluorescent increase at 552 nm induced by ssDNA 6mer is only 1.8-fold for the buffer solution of BTAESA. However, the remarkable enhancement of BTAESA fluorescence was recorded after mixed with longer ssDNA such as ssDNA 10mer, 15mer, 20mer, and 24mer. The fluorescent increase induced by ssDNA 10mer, 15mer, 20mer, and 24mer were up to 23-, 43-, 63-, and 80-fold in the buffer solution of BTAESA with the corresponding DNA, respectively. Therefore, longer ssDNA results in more significant fluorescence enhancement, as shown in Fig. 2b, and a linear range is observed from 6mer to 24mer ($R$ = 0.998). These results are comprehensible by considering the fact that long DNA will provide more negative charge sites for electrostatic interactions with the ammonium groups and nucleosides for hydrophobic interactions with aryl rings in BTAESA, thereby leading to strong aggregation of BTAESA. The short DNA can only offer limited negative sites and nucleosides for supramolecular interactions with BTAESA, and as a result, stable aggregation complex cannot be formed.

In fact, the fluorescent intensity of the ensemble was fluctuant and almost reached a plateau when the length of ssDNA exceeded 24mer. Therefore, the ensemble including 1.0 μM BTAESA and 400 nM aptamer ssDNA 24mer was used as a probing complex for the follow-up experiments.

Figure 2c shows the fluorescent changes of different concentrations of ssDNA 24mer using BTAESA as the indicator. When the concentration of ssDNA 24mer increases, the fluorescent intensity is enhanced, which indicates the aggregation complex of BTAESA, and ssDNA 24mer is expected to be formed. The variation of absorption spectrum of BTAESA in the absence and presence of ssDNA 24mer supports this assumption. As shown in Fig. 3, the buffer solution of BTAESA (33.7 μM) without addition of ssDNA 24mer shows the maximum absorption at 417 nm, and when ssDNA 24mer (4.0 μM) was added, the maximum absorption spectrum was red shifted to 431 nm, indicating the self-assembled aggregation of BTAESA. Figure 2d outlines the relationship between the fluorescence intensity at 552 nm and the concentration of ssDNA 24mer. A linear range is observed from 0 to 150 nM ($R$ = 0.998), and the fluorescent enhancement for BTAESA became rather small when the concentrations of ssDNA 24mer reached 400 nM. The detection limit could reach as low as 150 pM. Importantly, in the turn-on and label-free sensing mode, the easy preparation of BTAESA probe can offer additional advantages of this analytical approach.

## Sensing of S1 nuclease activity in real time

Many published articles reported that 37 °C was the optimum temperature for cleavage reaction process of ssDNA with S1

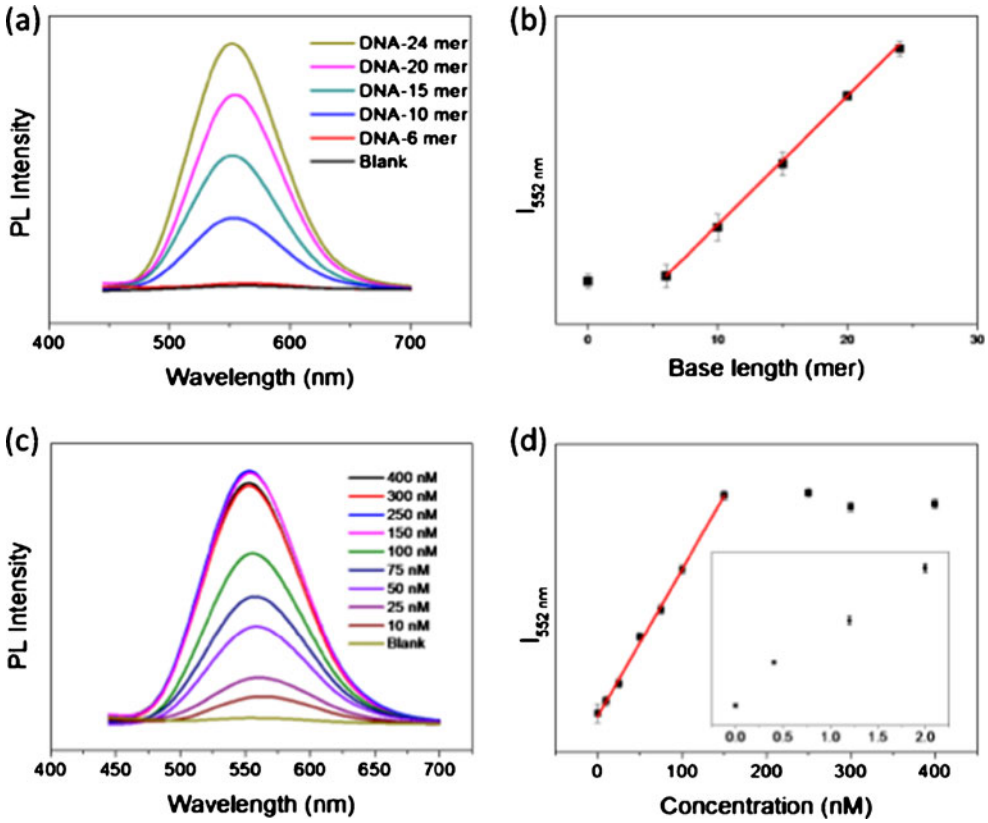


**Fig. 2** (**a**) Fluorescent spectra of BTAESA (1.0 μM in 20 mM Tris-HAc buffer solution, pH 7.2) in the presence of different length of ssDNAs (400 nM). (**b**) Change of the fluorescent spectra intensity of BTAESA at 552 nm with different lengths of ssDNAs. (**c**) Fluorescence spectra of BTAESA in the presence of different concentrations of ssDNA 24mer. (**d**) Change of the fluorescent spectra intensity of BTAESA at 552 nm with different concentrations of ssDNA 24mer. The *inset* shows a linear relationship in the low concentration range from 0.4 to 2.0 nM

nuclease [15, 50, 51]. We also found that 37 °C was the optimum temperature for the S1 nuclease activity based on the relative fluorescent intensity changes of BTAESA (see Electronic Supplementary Material Fig. S2). Herein, we chose 37 °C as the cleavage temperature for the follow-up experiments. Besides, the buffer for the experiments of S1 nuclease activity assay was 2 mM $CH_3COONa$, 15 mM NaCl, and 0.1 mM $ZnSO_4$, pH=4.6 [15, 52]. Under the optimal experimental conditions, S1 nuclease activity was detected by using the complex of BTAESA and ssDNA 24mer as the sensor. Figure 4a shows the variation of the relative fluorescence

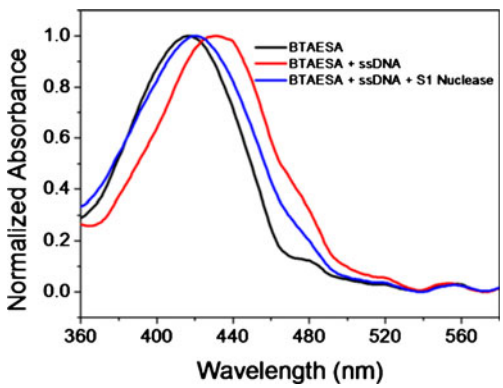


**Fig. 3** The absorption spectra of BTAESA (33.7 μM in 2 mM $CH_3COONa$, 15 mM NaCl, and 0.1 mM $ZnSO_4$, pH=4.6) in the absence (*black line*) and presence of ssDNA 24mer (4.0 μM) (*red line*) and ssDNA 24mer and S1 nuclease (320 U $ml^{-1}$) (*blue line*)

intensity of BTAESA (1.0 μM) at 552 nm with reaction time from 0 to 16 min. In the absence of S1 nuclease, it is found that the fluorescence remains constant over the period. However, the fluorescent intensity obviously decreased with the increase of S1 nuclease concentration over the range of 6–32 U $ml^{-1}$. This indicates that ssDNA 24mer was the substrate for S1 nuclease and could be effectively cleaved by S1 nuclease, and the DNA fragmentation could not induce aggregation of BTAESA effectively. Accordingly, the aggregation complex of BTAESA and ssDNA 24mer cannot be formed, because ssDNA 24mer fragments cannot induce the aggregation formation of BTAESA. The variation of absorption spectrum of BTAESA in the presence of ssDNA 24mer and S1 nuclease supports this assumption. As shown in Fig. 3, the complex of BTAESA and ssDNA 24mer shows the maximum absorption at 431 nm. After addition of S1 nuclease (320 U $ml^{-1}$), the maximum absorption spectrum was blue shifted to 420 nm, which indicates that the change of absorption spectral should be owing to the disaggregation of BTAESA. Besides, the fluorescent intensity of the biosensor with various concentrations of S1 nuclease became distinguishable within 3–16 min. Therefore, it was possible to assay of the enzyme activity within 3–16 min, which showed the advantage of quick response of the biosensor.

The reaction rate which enhanced with the increase of enzyme concentration and the initial digestion rate ($V_0$) can be measured from the amount of ssDNA 24mer remaining in the mixture before and after cleavage of 13 min. As shown in

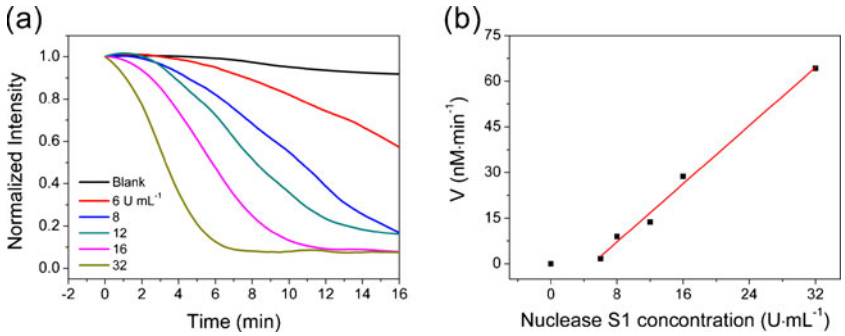


**Fig. 4** Fluorescent sensing of the ssDNA 24mer (400 nM) cleavage by S1 nuclease. (**a**) Normalized fluorescent intensity of BTAESA (1.0 μM in 2 mM $CH_3COONa$, 15 mM NaCl, and 0.1 mM $ZnSO_4$, pH=4.6) at 552 nm with various concentrations of S1 nuclease at 37 °C. The concentrations of S1 nuclease from the *top to bottom* were 0, 6, 8, 12, 16, and 32 U $ml^{-1}$. (**b**) The linear relation between the initial cleavage reaction rate and the concentration of S1 nuclease

Fig. 4b, a linear correlation ($R$=0.995) was observed between $V_0$ and the concentration of S1 nuclease over the range of 6–32 U $ml^{-1}$. In addition, 6 U $ml^{-1}$ of S1 nuclease could be clearly detected after the cleavage of 16 min, and more sensitive assay could be expected by increasing the concentration of ssDNA 24mer or prolonging the enzyme-catalyzed reactions time.

To test the specificity of this ssDNA biosensor, interference dsDNA (calf thymus DNA, ctDNA) was investigated. There was no obvious changes in the fluorescent peak intensity of BTAESA/dsDNA after digestion for 10 min by S1 nuclease (see Electronic Supplementary Material Fig. S3), because S1 nuclease is a single-strand-specific endonuclease, and the duplex structure of dsDNA could block the hydrolysis digestion of S1 nuclease; the aggregation complex of BTAESA and undigested dsDNA is expected to be formed when BTAESA is added due to the electrostatic interactions between ammonium cations of BTAESA and the backbone negative phosphate anions of dsDNA and the possible hydrophobic interaction between nucleosides and aryl rings in BTAESA, demonstrating the good selectivity of the proposed biosensor for ssDNA over dsDNA.

In addition, the repeatability and reproducibility of the biosensor are measured according to the same procedure. The relative standard deviation (R.S.D.) of the sensor response to 32 U $ml^{-1}$ S1 nuclease is 2.5 % for nine successive measurements, demonstrating that the complex of BTAESA and ssDNA 24mer can be used repeatedly for the sensing of S1 nuclease. The fabrication reproducibility of seven sensors, made independently, shows reproducibility with the R.S.D. of 3.0 % for a 32-U $ml^{-1}$ S1 nuclease, confirming that the fabrication method is reproducible.

## Sensing of S1 nuclease inhibition

Under the optimal experimental conditions, the cleavage reaction of ssDNA 24mer by S1 nuclease can be prohibited when the nuclease inhibitor is present. Since the cleavage reaction can be detected on the basis of the fluorescent change of BTAESA, the probe also can be employed for nuclease inhibitors screening. By taking $Na_2ATP$ as an example, which is known as the effective inhibitor to prevent the cleavage of ssDNA 24mer with S1 nuclease, we used the BTAESA for evaluating the prohibition effect on S1 nuclease. Figure 5a shows the changes of the fluorescent intensity of BTAESA/ssDNA 24mer complex in the presence of S1 nuclease with 32 U $ml^{-1}$ and different concentrations of $Na_2ATP$. In the absence of $Na_2ATP$, the fluorescent intensity of the complex

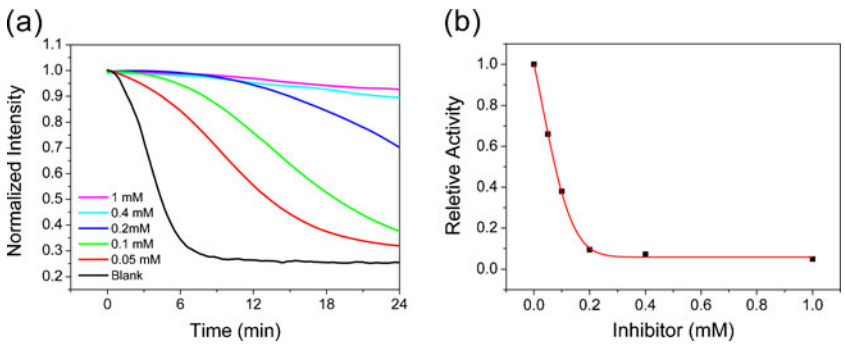


**Fig. 5** Fluorescent sensing of the inhibition effect with $Na_2ATP$. (**a**) Normalized fluorescent intensity of BTAESA/ssDNA 24mer complex at 552 nm with different concentrations of $Na_2ATP$ in the presence of 32 U $ml^{-1}$ S1 nuclease at 37 °C. [BTAESA]=1.0 μM, [ssDNA 24mer]=400 nM, the concentrations of $Na_2ATP$ from the *bottom to top* were 0, 0.05, 0.1, 0.2, 0.4, and 1 mM. (**b**) Inhibition efficiency of S1 nuclease activity by $Na_2ATP$

obviously decreased with increasing reaction time, indicating that the cleavage reaction proceeded well. In the presence of different concentrations of $Na_2ATP$, however, the extent of fluorescent recovery increased gradually with increasing $Na_2ATP$, implying that the cleavage reaction by S1 nuclease was prohibited. The digestion of ssDNA 24mer by S1 nuclease is effectively inhibited by $Na_2ATP$ at the concentration of 0.4 mM (Fig. 5b). Besides, $Na_2ATP$ was found to inhibit S1 nuclease with $IC_{50}$ values (the inhibitor concentration required to reduce enzyme activity by 50 %) of 0.076 mM. The result is inconsistent with the fact that $Na_2ATP$ is known as the inhibitor of S1 nuclease, and therefore, these results further demonstrate that as a novel fluorescent biosensor, BTAESA/ssDNA 24mer complex can be used not only for label-free fluorescent nuclease activity sensing but also for turn-on assay of nuclease inhibitors in real time.

## Conclusions

In summary, a 9,10-distyrylanthracene derivative with two ammonium groups (BTAESA) was designed and synthesized to develop a new optical probe. Besides, we have constructed a novel biosensor employing on our probe and single-strands desoxyribonucleic acid for real-time sensing of nuclease activity and inhibition based on the controlled self-assembly of AIE-active BTAESA probe. The assay present here was simple in design and offered a convenient protocol for homogeneous, real-time, and label-free determination with high sensitivity. Experiment results clearly indicate that BTAESA can be used for fluorescence turn-on sensing of DNA. For ssDNA 24mer, the detection limit can reach 150 pM by BTAESA. Besides, S1 nuclease activity could be quantitatively monitored in real time by the value of velocity of the nuclease reaction monitored, and 6 U $ml^{-1}$ can be apparently detected by our biosensor. Furthermore, this AIE-based biosensor shows a potential application for fluorescence turn-on and high-throughput screening of nuclease inhibitors. We expect that this AIE-based technology will have a critical application in the fields of biological and biomedical processes, therapeutic agents, and medical diagnostics.

**Acknowledgments** This work was supported by 973 Program (2013CB834702, 2009CB623605), the Natural Science Foundation of China (nos. 21074045 and 21204027), the Research Fund for the Doctoral Program of Higher Education of China (20120061120016), and the Project of Jilin Province (20100704).

## References

1. Arber W (1978) Angew Chem Int Ed 17(2):73–79
2. Lieber MR (1997) BioEssays 19(3):233–240
3. Pingoud A, Jeltsch A (2001) Nucleic Acids Res 29(18):3705–3727
4. Grindley NDF, Whiteson KL, Rice PA (2006) Mechanisms of site-specific recombination. Annual Review of Biochemistry 75:567–605. doi:10.1146/annurev.biochem.73.011303.073908
5. West SC (2003) Nat Rev Mol Cell Biol 4(6):435–445
6. Norberg P, Bergstrom T, Liljeqvist J-A (2006) J Clin Microbiol 44(12):4511–4514
7. Polisky B, Greene P, Garfin DE, McCarthy BJ, Goodman HM, Boyer HW (1975) PNAS 72(9):3310–3314
8. McLaughlin LW, Benseler F, Graeser E, Piel N, Scholtissek S (1987) Biochemistry 26(23):7238–7245
9. Halford SE, Goodall AJ (1988) Biochemistry 27(5):1771–1777
10. Windolph S, Fritz A, Oelgeschläger T, Wolfes H, Alves J (1997) Biochemistry 36(31):9478–9485
11. VanderVeen LA, Druckova A, Riggins JN, Sorrells JL, Guengerich FP, Marnett LJ (2005) Biochemistry 44(13):5024–5033
12. Fliess A, Wolfes H, Rosenthal A, Schwellnus K, Blöcker H, Frank R, Pingoud A (1986) Nucleic Acids Res 14(8):3463–3474
13. Biagiotti V, Porchetta A, Desiderati S, Plaxco KW, Palleschi G, Ricci F (2012) Anal Bioanal Chem 402(1):413–421
14. Jeltsch A, Fritz A, Alves J, Wolfes H, Pingoud A (1993) Anal Biochem 213(2):234–240
15. Tang Y, Feng F, He F, Wang S, Li Y, Zhu D (2006) J Am Chem Soc 128(46):14972–14976
16. Xu X, Han MS, Mirkin CA (2007) Angew Chem Int Ed 46(19): 3468–3470
17. Yang Y, Li W, Qi H, Zhang Q, Chen J, Wang Y, Wang B, Wang S, Yu C (2012) Anal Biochem 430(1):48–52
18. Shen Q, Nie Z, Guo M, Zhong C-J, Lin B, Li W, Yao S (2009) Chem Commun (8):929–931
19. Ray PC, Fortner A, Darbha GK (2006) J Phys Chem B 110(42): 20745–20748
20. Li X, Zhu S, Xu B, Ma K, Zhang J, Yang B, Tian W (2013) Nanoscale 5(17):7776–7779
21. Luo J, Xie Z, Lam JW, Cheng L, Chen H, Qiu C, Kwok HS, Zhan X, Liu Y, Zhu D, Tang BZ (2001) Chem Commun (Camb) (18):1740–1741
22. Tong H, Hong Y, Dong Y, Haeussler M, Lam JWY, Li Z, Guo Z, Guo Z, Tang BZ (2006) Chem Commun (35):3705–3707
23. Hong Y, Lam JWY, Tang BZ (2009) Chem Commun (29):4332–4353
24. Hong Y, Lam JWY, Tang BZ (2011) Chem Soc Rev 40(11):5361–5388
25. Zhao G, Shi C, Guo Z, Zhu W, Zhu S (2012) Chin J Org Chem 32(9): 1620–1632
26. Wu J, Liu W, Ge J, Zhang H, Wang P (2011) Chem Soc Rev 40(7): 3483–3495
27. Shi H, Kwok RTK, Liu J, Xing B, Tang BZ, Liu B (2012) J Am Chem Soc 134(43):17972–17981
28. Shi H, Liu J, Geng J, Tang BZ, Liu B (2012) J Am Chem Soc 134(23):9569–9572
29. Hong Y, Häuβler M, Lam JWY, Li Z, Sin KK, Dong Y, Tong H, Liu J, Qin A, Renneberg R, Tang BZ (2008) Chem Eur J 14(21):6428–6437
30. Huang J, Wang M, Zhou Y, Weng X, Shuai L, Zhou X, Zhang D (2009) Bioorg Med Chem 17(22):7743–7748
31. Hong Y, Xiong H, Lam JWY, Häußler M, Liu J, Yu Y, Zhong Y, Sung HHY, Williams ID, Wong KS, Tang BZ (2010) Chem Eur J 16(4): 1232–1245
32. Wang M, Zhang D, Zhang G, Tang Y, Wang S, Zhu D (2008) Anal Chem 80(16):6443–6448
33. An B-K, Kwon S-K, Jung S-D, Park SY (2002) J Am Chem Soc 124(48):14410–14415
34. Yeh H-C, Yeh S-J, Chen C-T (2003) Chem Commun (20):2632–2633
35. Xu B, Chi Z, Zhang J, Zhang X, Li H, Li X, Liu S, Zhang Y, Xu J (2011) Chem Asian J 6(6):1470–1478

36. Chen S, Hong Y, Liu Y, Liu J, Leung CWT, Li M, Kwok RTK, Zhao E, Lam JWY, Yu Y, Tang BZ (2013) J Am Chem Soc 135(13):4926–4929
37. Hong Y, Meng L, Chen S, Leung CWT, Da L-T, Faisal M, Silva D-A, Liu J, Lam JWY, Huang X, Tang BZ (2012) J Am Chem Soc 134(3): 1680–1689
38. Leung CWT, Hong Y, Chen S, Zhao E, Lam JWY, Tang BZ (2013) J Am Chem Soc 135(1):62–65
39. Luo Z, Yuan X, Yu Y, Zhang Q, Leong DT, Lee JY, Xie J (2012) J Am Chem Soc 134(40):16662–16670
40. Wang Z, Xu B, Zhang L, Zhang J, Ma T, Zhang J, Fu X, Tian W (2013) Nanoscale 5(5):2065–2072
41. Lu H, Xu B, Dong Y, Chen F, Li Y, Li Z, He J, Li H, Tian W (2010) Langmuir 26(9):6838–6844
42. Li X, Xu B, Lu H, Wang Z, Zhang J, Zhang Y, Dong Y, Ma K, Wen S, Tian W (2013) Anal Methods 5(2):438–441
43. Lu H, Su F, Mei Q, Zhou X, Tian Y, Tian W, Johnson RH, Meldrum DR (2012) J Polym Sci A Polym Chem 50(5):890–899
44. Si N, Matsuda K, Uesugi Y, Nakashima K, Akiyama S, Katzer G, Fabian W (1991) J Chem Soc Perkin Trans 2(6):861–867
45. Solntsev KM, McGrier PL, Fahrni CJ, Tolbert LM, Bunz UHF (2008) Org Lett 10(12):2429–2432
46. Duan X, Liu L, Feng F, Wang S (2009) Acc Chem Res 43(2):260–270
47. Deng J, Jin Y, Chen G, Wang L (2012) Analyst 137(7):1713–1717
48. Liu J, Lu Y (2003) Anal Chem 75(23):6666–6672
49. Chen X, Guan H, He Z, Zhou X, Hu J (2012) Anal Methods 4(6): 1619–1622
50. Svobodova M, Pinto A, Nadal P, O'Sullivan C (2012) Anal Bioanal Chem 404(3):835–842
51. Mohamed D, Linscheid M (2008) Anal Bioanal Chem 392(5):805–817
52. Yang X, Pu F, Ren J, Qu X (2011) Chem Commun 47(28):8133–8135